

Magnetization induced dynamics of a Josephson junction coupled to a nanomagnet

Roopayan Ghosh⁽¹⁾, Moitri Maiti⁽²⁾, Yury M. Shukrinov,^(2,3) and K. Sengupta⁽¹⁾

⁽¹⁾ *Theoretical Physics Department, Indian Association for the Cultivation of Science, Jadavpur, Kolkata-700032, India.*

⁽²⁾ *BLTP, JINR, Dubna, Moscow region, 141980, Russia*

⁽³⁾ *Dubna State University, Dubna, Russian Federation.*

(Dated: May 26, 2022)

We study the current-voltage (I-V) characteristics of a Josephson junction (JJ) coupled to an external nanomagnet driven by a time dependent magnetic field both without and in the presence of an external AC drive. We provide an analytic solution for the Landau-Lifshitz (LL) equations governing the coupled JJ-nanomagnet system in the presence of a magnetic field with arbitrary time-dependence oriented along the easy axis of the nanomagnet's magnetization and in the limit of weak dimensionless coupling ϵ_0 between the JJ and the nanomagnet. We show the existence of Shapiro-like steps in the I-V characteristics of the JJ for a constant or periodically varying magnetic field and explore the effect of rotation of the magnetic field and the presence of an external AC drive on these steps. We support our analytic results with exact numerical solution of the LL equations. We also extend our results to dissipative nanomagnets by providing a perturbative solution to the Landau-Lifshitz-Gilbert (LLG) equations for weak dissipation. We study the fate of magnetization-induced Shapiro steps in the presence of dissipation both from our analytical results and via numerical solution of the coupled LLG equations. We discuss experiments which can test our theory.

PACS numbers: 03.75.Lm, 05.30.Jp, 05.30.Rt

I. INTRODUCTION

The physics of Josephson junctions (JJs) has been the subject of intense theoretical and experimental endeavor for decades¹. The interest in the physics of such JJs has received renewed attention in recent years in the context of Majorana modes in unconventional superconductors²⁻⁵. Indeed, it has been theoretically predicted^{2,3} and experimentally observed⁶ that such junctions may serve as a test bed for detection of Majorana end modes in unconventional superconductors. It has been shown that the presence of such end modes lead to fractional Josephson effect^{2,3} and results in the absence of odd Shapiro steps⁷ when such junctions are subjected to an external AC drive⁸⁻¹⁰.

Another interesting phenomenon which has been extensively studied in context of JJs is their current-voltage (I-V) characteristics in the presence of a finite coupling to a nanomagnet. The physics of such a JJ-nanomagnet system has been theoretically studied in Refs. 11,12, where the effects of spin-flip of the nanomagnet on the Josephson current was charted out. More recently, there has been several theoretical studies on a variety of aspects of such systems including effect of superconducting correlations on the spin dynamics of the nanomagnet¹³, the influence of spin-orbit coupling of a single spin on the Josephson current¹⁴, and the effect of deposition of single magnetic molecules on superconducting quantum interference devices (SQUIDS) made out of such junctions¹⁵. Another interesting phenomenon which has been widely studied in this context is magnetization switching^{16,17} which constitutes magnetization reversal of the nanomagnet by an externally driven JJ. Such theoretical studies were complemented by experimental work on these

systems¹⁸. More recently, the possibility of magnetization reversal of a single spin using a JJ subjected to a static field and a weak linearly polarized microwave radiation has been demonstrated in Ref. 19. The possibility of the presence of Shapiro-like steps in the I-V characteristics of such coupled JJ-nanomagnet for constant applied magnetic field has also been pointed out in Ref. 16. However, to the best of our knowledge, the current-voltage (I-V) characteristics of a JJ in the presence of a nanomagnet with time-dependent magnetic fields and in the presence of external AC drive has not been studied systematically so far.

In this work we study a JJ coupled to a nanomagnet with a fixed easy-axis anisotropy direction (chosen to be \hat{y}) in the presence of an arbitrary time dependent external magnetic field along \hat{y} . For nanomagnets with weak anisotropy, we find an analytic perturbative solution to the coupled Landau-Lifshitz (LL) equations in the limit of weak coupling between the nanomagnet and the JJ. Using this solution, we show that a finite DC component of the supercurrent leading to Shapiro-like steps in the I-V characteristics of the JJ, can occur for either a constant or a periodically time dependent magnetic field. Our theoretical analysis provides exact analytic results for the position of such steps. We study the stability of these steps against change in the direction of the applied magnetic field and increase of the dimensionless coupling strength ϵ_0 between the JJ and the nanomagnet. We also provide a detailed analysis of the fate of this phenomenon in the presence of an external AC drive and demonstrate that the presence of such a drive leads to several new fractions (ratio between the applied DC voltage and the drive frequency) at which the supercurrent develops a finite DC component leading to Shapiro steps in the I-V characteristics. We support our analytical results with

numerical study of the systems which allows exact, albeit numerical, investigation of the dynamics of the coupled JJ and nanomagnet system. We also extend our study to systems with dissipation via perturbative analytic and exact numerical solution of the coupled Landau-Lifshitz-Gilbert (LLG) equations and study the behavior of the steps with increasing dissipation. Finally, we discuss experiments which may test our theory.

The plan of the rest of this work is as follows. In Sec. II, we provide the analytic solution of the LL equations governing the coupled nanomagnet and JJ. This is followed by an analogous solution for LLG equations describing the coupled JJ-nanomagnet system in the presence of dissipation in Sec. II C. Next, in Sec. III, we back the analytical results with exact numerics and discuss details of Shapiro-step like features in the I-V of the JJ for constant or periodic magnetic field. Finally, we chart out our main results, discuss experiments which can test our theory, and conclude in Sec. IV.

II. FORMALISM AND ANALYTICAL SOLUTION

In this section, we obtain analytic solution to the LL equations for the weakly coupled JJ-nanomagnet system. We shall sketch the general derivation of our result for arbitrary time-dependent magnetic field in Sec. II A and then apply these results to demonstrate the existence of Shapiro-like steps for constant and periodic magnetic fields in Sec. II B. The extension of these results for dissipative magnets will be charted out in Sec. II C.

A. Perturbative solution

The coupled JJ-nanomagnet system is schematically shown in Fig. 1. In what follows we consider a 2D JJ along \hat{x} and choose the easy axis of the nanomagnet along \hat{y} ; the radius vector \vec{r} between the nanomagnet and the JJ thus lies in the $x - y$ plane as shown in Fig. 1. The energy functional governing the JJ and the nanomagnet is given by¹⁶

$$\begin{aligned} E &= E_1 + E_2 \\ E_1 &= -KM_y^2 - M_y B(t), \quad E_2 = -E_J \cos \gamma, \end{aligned} \quad (1)$$

where $K > 0$ denotes the magnetization anisotropy constant, $\vec{B}(t) \parallel \hat{y}$ is the external magnetic field which can have arbitrary time dependence, and E_J is the Josephson energy of the junction. The phase difference γ across the junction is given by

$$\begin{aligned} \gamma(t) &= \gamma_0(t) + \gamma_1(t), \\ \gamma_0(t) &= \gamma_{00} + \frac{2e}{\hbar} \int^t V_0(t') dt' = \gamma_{00} + \omega'_0 \int^t g(t') dt' \\ \gamma_1(t) &= -\frac{2\pi}{\Phi_0} \int \vec{dl} \cdot \vec{A}(\vec{r}), \end{aligned} \quad (2)$$

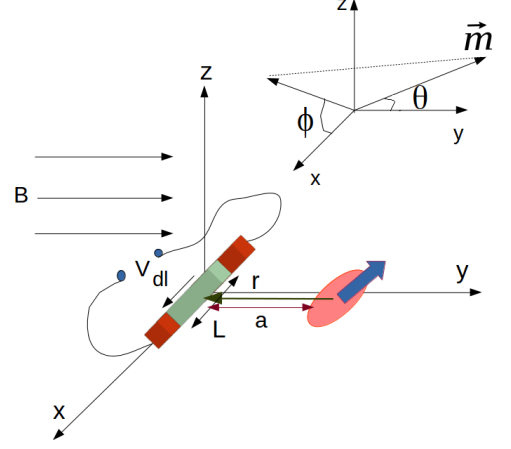


FIG. 1: A schematic representation of the JJ-nanomagnet system showing the position of the nanomagnet (shown schematically by the filled oval and an arrow representation the direction of its magnetization) and the JJ along with the direction of the magnetic field. The inset shows the angles θ and ϕ used to specify the direction of the nanomagnet's magnetization $\vec{m} = \vec{M}/|\vec{M}|$.

where γ_{00} is the intrinsic DC phase of the JJ, γ_0 is the phase generated by the external voltage, $V_0(t) = V_0 g(t)$ is the applied voltage across it, $\omega'_0 = 2eV_0/\hbar$ is the Josephson frequency of the junction, $g(t)$ is a dimensionless time dependent function specifying the time dependence of the applied magnetic field, $\Phi_0 = \hbar c/2e$ is the flux quantum, e is the charge of an electron, and c is the speed of light. The vector potential $\vec{A}(\vec{r})$ is given by

$$\vec{A}(\vec{r}, t) = \mu_0(\vec{M}(t) \times \vec{r})/(4\pi|\vec{r}|^3). \quad (3)$$

Note that in our chosen geometry, as shown in Fig. 1, $\vec{dl} \parallel \hat{x}$ and \vec{r} lies in the $x - y$ plane, so that

$$\begin{aligned} \gamma_1(t) &= -k_0 M_z(t)/|\vec{M}|, \\ k_0 &= \mu_0 |\vec{M}| l / (2\Phi_0 a \sqrt{l^2 + a^2}), \end{aligned} \quad (4)$$

where the geometrical factor k_0 can be tuned by tuning the distance a between the JJ with the nanomagnet (Fig. 1). Moreover, in this geometry, the orbital effect of the magnetic field do not affect the phase of the JJ since $A_B \sim \vec{dl} \cdot (\vec{B} \times \vec{r}) = 0$. In this geometry, the LL equations for the nanomagnet reads

$$\begin{aligned} \frac{d\vec{M}}{dt} &= \gamma_g(\vec{M} \times \vec{B}_{\text{eff}}) \\ \vec{B}_{\text{eff}} &= -\frac{\delta E}{\delta \vec{M}} = B(M_y)\hat{y} + \frac{E_J k_0}{|\vec{M}|} \sin(\gamma_0(t) + \gamma_1(t))\hat{z} \end{aligned} \quad (5)$$

where $B(M_y) = KM_y + B(t)$ and γ_g is the gyromagnetic ratio. We note that the LL equation are to be solved along with the constraint of constant $|\vec{M}|$; in what follows we shall set $|\vec{M}| = M_0$.

Eq. 5 represents a set of non-linear equations which, in most cases, need to be solved numerically. Here we identify a limit in which these equations admits an analytic solution for arbitrary $B(t)$. To this end we define the following dimensionless quantities

$$\begin{aligned}\vec{m} &= \vec{M}/M_0 = (\sin \theta \cos \phi, \cos \theta, \sin \theta \sin \phi) \\ \omega_B(t) &= B(M_y)/B_1, \quad \epsilon_0 = k_0 E_J/(B_1 M_0) \\ B(t) &= B_1 f(t), \quad t' = \gamma_g B_1 t, \quad \omega_0 = \omega'_0/(\gamma_g B_1)\end{aligned}\quad (6)$$

where $f(t)$ is a arbitrary dimensionless function, ω_0 is the dimensionless Josephson frequency, and B_1 is the amplitude of the external magnetic field. In what follows we shall seek perturbative solution for \vec{m} in the weak coupling and weak anisotropy limit (for which $\epsilon_0, KM_0/B_1 \ll 1$ and $k_0 \leq 1$) to first order in ϵ_0 and K . In terms of the scaled variables, the LL equations (Eq. 5) can be written in terms of θ and ϕ as

$$\begin{aligned}\frac{d\phi}{dt'} &= \omega_B(t') - \epsilon_0 \cot \theta \sin \phi \sin(\gamma_0(t') - k_0 \sin \theta \sin \phi) \\ \frac{d\theta}{dt'} &= \epsilon_0 \cos \phi \sin(\gamma_0(t') - k_0 \sin \theta \sin \phi).\end{aligned}\quad (7)$$

with the initial condition $\phi(t' = 0) = 0$ and $\theta(t' = 0) = \theta_0$. We note that the choice of this initial condition for θ and ϕ amounts to choosing the initial magnetization of the nanomagnet in the $x-y$ plane: $\vec{M} = (M_1, M_2, 0)$ where $\cos \theta_0 = M_2/M_0$, and $M_1^2 + M_2^2 = M_0^2$. We choose θ_0 such that $\cot \theta_0 < 1$ and the perturbative solutions that we present remains valid as long as $\epsilon_0 \cot(\theta) \ll 1$. We have checked that this limit is satisfied in all our numerical simulations described in Sec. III.

The perturbative solutions of Eq. 7 can be obtained by writing

$$\begin{aligned}\theta(t') &= \delta\theta(t'), \quad \phi(t') = z(t') + \delta\phi(t') \\ z(t') &= K \cos(\theta_0) M_0 t' / B_1 + \int_0^{t'} d\tau f(\tau)\end{aligned}\quad (8)$$

where $\delta\theta(t')$ and $\delta\phi(t')$ satisfies, to first order in ϵ_0 and K [i.e., neglecting terms $O(\epsilon_0^2)$, $O(K\epsilon_0)$ and $O(k_0\epsilon_0)$],

$$\begin{aligned}\frac{d\delta\phi}{dt'} &= -\epsilon_0 \cot(\theta_0) \sin(z(t')) \\ &\quad \times \sin(\gamma_0(t') - k_0 \sin(\theta_0) \sin(z(t'))) \\ \frac{d\delta\theta}{dt'} &= \epsilon_0 \cos(z(t')) \sin(\gamma_0(t') - k_0 \sin(\theta_0) \sin(z(t'))).\end{aligned}\quad (9)$$

The solution of Eq. 9 is straightforward and can be written as

$$\begin{aligned}\delta\theta(t') &= \epsilon_0 \int_0^{t'} d\tau [\cos(z(\tau)) \sin[\gamma_0(\tau) \\ &\quad - k_0 \sin(\theta_0) \sin(z(\tau))]] \\ \delta\phi(t') &= -\epsilon_0 \cot \theta_0 \int_0^{t'} d\tau [\sin(z(\tau)) \sin[\gamma_0(\tau) \\ &\quad - k_0 \sin(\theta_0) \sin(z(\tau))]]\end{aligned}\quad (10)$$

Eqs. 8, 9, and 10 constitute the central result of this work. These equations describe the dynamics of a nanomagnet in the presence of weak coupling with a JJ. We note that in obtaining these results, we have neglected the normal state resistance of the JJ which can be safely done for tunnel junctions or for weak links with large resistance and small capacitance¹⁶. We also note that the domain of validity of these solutions require $\delta\theta(t'), \delta\phi(t') \leq z(t')$ at all times; we shall discuss this domain in the context of specific drives in Sec. IIB. We now use these solutions to study the behavior of the supercurrent of the JJ given by

$$I_s = I_c \sin[\gamma_0(t') - k_0 \sin(\phi(t')) \sin(\theta(t'))] \quad (11)$$

for several possible magnetic field profiles. Here I_c is the critical current of the JJ. Although Eq. 11 yields I_s for any magnetic field profile, in what follows we shall concentrate on constant and periodically varying magnetic fields since they allow for Shapiro-step like features in the I-V characteristics.

Before ending this subsection, we note that the solutions for \vec{M} is stable against small fluctuations of the direction of the applied magnetic field. To see this, we write the external magnetic field \vec{B} is applied in an arbitrary direction in the $x-y$ plane: $\vec{B} = B_1 f(t)(\sin(\alpha_0), \cos(\alpha_0), 0)$ with $K\alpha_0 \ll K$. Next, we move to a rotated coordinate frame for which the magnetization \vec{m}' is related to \vec{m} by

$$\begin{pmatrix} m'_x \\ m'_y \\ m'_z \end{pmatrix} = \begin{pmatrix} \cos \alpha_0 & -\sin \alpha_0 & 0 \\ \sin \alpha_0 & \cos \alpha_0 & 0 \\ 0 & 0 & 1 \end{pmatrix} \begin{pmatrix} m_x \\ m_y \\ m_z \end{pmatrix} \quad (12)$$

We proceed by using the parametrization $\vec{m}' = (\sin \theta' \cos \phi', \cos \theta', \sin \theta' \sin \phi')$. In this representation, the initial values of \vec{m}' are given by

$$m'_x(t=0) = \sin(\theta_0 - \alpha_0), \quad m'_y = \cos(\theta_0 - \alpha_0), \quad m'_z = 0 \quad (13)$$

where θ_0 and $\phi_0 = 0$ depicts the initial condition for \vec{m} . Next, repeating the same algebraic steps as outlined earlier in the section, one finds that the equations governing θ' and ϕ' are given by

$$\begin{aligned}\frac{d\theta'}{dt'} &= \epsilon_0 \cos(\phi') \sin(\gamma_0(t') - k \sin(\theta') \sin(\phi')) \\ \frac{d\phi'}{dt'} &= \omega'_B - \epsilon_0 \cot(\theta') \sin(\phi') \\ &\quad \times \sin(\gamma_0(t') - k_0 \sin(\theta') \sin(\phi')) \\ \omega'_B &= K(\cos(\alpha_0) \cos(\theta') + \sin(\alpha_0) \sin(\theta') \sin(\phi'))/B_1 \\ &\quad + f(t') \simeq \omega_B(t') + O(K\alpha_0)\end{aligned}\quad (14)$$

Note that the analytic solution to Eq. 15 can only be obtained when terms $O(K\alpha_0)$ can be neglected. In this case, the perturbative solution to Eq. 15 can be obtained in the same way as done before in this section. The final

result is

$$\begin{aligned}
\theta'(t') &= \delta\theta'(t'), \quad \phi'(t') = z(t') + \delta\phi'(t') \\
\delta\theta(t') &= \epsilon_0 \int_0^{t'} d\tau [\cos(z(\tau)) \sin[\gamma_0(\tau) \\
&\quad - k_0 \sin(\theta_0 - \alpha_0) \sin(z(\tau))]] \\
\delta\phi(t') &= -\epsilon_0 \cot \theta_0 \int_0^{t'} d\tau [\sin(z(\tau)) \sin[\gamma_0(\tau) \\
&\quad - k_0 \sin(\theta_0 - \alpha_0) \sin(z(\tau))]] \quad (16)
\end{aligned}$$

The behavior of these solutions shall be checked against exact numerics in Sec. III.

B. Constant and Periodically varying magnetic fields

In this section, we apply our perturbative results on constant and periodically time-varying magnetic fields for which the I-V characteristics of the JJ may have Shapiro-like steps. While this effect has been discussed, using a somewhat different geometry, in Ref. 16 for constant magnetic field, we demonstrate its presence for periodic magnetic fields.

Constant magnetic field: This case was studied in Ref. 16. For this $g(t) = 1$ and one $\gamma_0 = \omega_0 t' + \gamma_{00}$, where γ_{00} is the phase difference across the JJ at $t = 0$. Further, in this case, $f(t) = 1$, and $z(t') = \omega_B t'$. Thus the supercurrent to the leading order and for $\epsilon_0, K \ll 1$, is given by

$$\begin{aligned}
I_s &\simeq I_c \sin(\omega_0 t' + \gamma_{00} - k_0 \sin(\theta_0) \sin(\omega_B t')) \\
&= I_c \sum_n J_n[k_0 \sin(\theta_0)] \sin[(\omega_0 - n\omega_B)t' + \gamma_{00}] \quad (17)
\end{aligned}$$

which indicates the presence of a finite DC component of I_s leading to Shapiro steps in the I-V characteristics of the JJ-nanomagnet system at

$$\omega_0 = n^0 \omega_B. \quad (18)$$

To study the stability of these steps we consider the solution to $O(\epsilon_0)$. For constant magnetic field, the $O(\epsilon_0)$ correction to \vec{M} can be obtained from Eq. 10 which, after some straightforward algebra, yields for $z(t) = \omega_B t$

$$\begin{aligned}
\delta\theta(t') &= -\epsilon_0 \sum_n J_n(k_0 \sin(\theta_0)) \\
&\quad \times \sum_{s=\pm 1} \frac{\cos[(\omega_0 - (n-s)\omega_B)t' + \gamma_{00}] - \cos \gamma_{00}}{\omega_0 - (n-s)\omega_B} \\
\delta\phi(t') &= \epsilon_0 \cot(\theta_0) \sum_n J_n(k_0 \sin(\theta_0)) \quad (19) \\
&\quad \times \sum_{s=\pm 1} s \frac{\sin[(\omega_0 - (n-s)\omega_B)t' + \gamma_{00}] - \sin \gamma_{00}}{\omega_0 - (n-s)\omega_B}
\end{aligned}$$

We note that for $n = n_{\pm}$ which satisfies $n_0 = n_{\pm} \pm 1$, both $\delta\theta$ and $\delta\phi$ grows linearly in time. These terms turn out to be the most important corrections to the zeroth order solution near $\omega_0 = n^0 \omega_B$ and leads to the destabilization of the steps as ϵ_0 increases. We also note that such terms restrict validity of the perturbative expansion up to a finite time T_p so that $\epsilon_0 \cot(\theta_0) J_{n_{\pm}}(k \sin(\theta_0)) T_p \sim 1$; we shall discuss this in more details while comparing our perturbative results with exact numerics in Sec. III. The supercurrent to first order in ϵ_0 and K is thus given by

$$I_s \simeq I_c \sin(\omega_0 t' - k_0 \sin(\theta_0 + \delta\theta(t')) \sin(\omega_B t' + \delta\phi(t'))) \quad (20)$$

The behavior of the DC component of I_s in the presence of these corrections is charted out in Sec. III.

Periodic Magnetic fields: In this case, we choose a periodic magnetic field so that $f(t') = \cos(\omega_1 t')$, where ω_1 is the external drive frequency measured in units of $\gamma_g B_1$. For this choice, one has $z(t') = \omega_2 t' + \sin(\omega_1 t')/\omega_1$, where $\omega_2 = \gamma_g K M_2/B_1$. Thus the zeroth order solution for the supercurrent I_s^{periodic} reads

$$\begin{aligned}
I_s^{\text{periodic}} &\simeq I_c \sin[\omega_0 t' + \gamma_{00} - k_0 \sin(\theta_0) \\
&\quad \times \sin(\omega_2 t' + \sin(\omega_1 t')/\omega_1)] \\
&= I_c \sum_{n_1, n_2} J_{n_1}(k_0 \sin(\theta_0)) J_{n_2}(n_1/\omega_1) \\
&\quad \times \sin[\gamma_{00} + (\omega_0 - n_2 \omega_1 - n_1 \omega_2)t]. \quad (21)
\end{aligned}$$

We note that this solution admits a finite DC component of I_s^{periodic} and hence Shapiro-like steps for $(n_1, n_2) = (n_1^0, n_2^0)$ for which

$$\omega_0 - n_2^0 \omega_1 - n_1^0 \omega_2 = 0. \quad (22)$$

The amplitude of these peaks depend on product of two Bessel functions unlike the ones found for constant magnetic field¹⁶; moreover, the condition for their occurrence depends on two distinct integers which allows the peaks to occur in the absence of any DC voltage across the junction. The condition for occurrence of such peaks are given by $\omega_0 = 0$ and $\omega_2 = n_2^0 \omega_1/n_1^0$; they provide examples of Shapiro steps without any voltage bias across a JJ and have no analog in their constant magnetic field counterparts.

The first order corrections to these solutions can be obtained in a manner analogous to one used for constant magnetic field. The final result is given by

$$\begin{aligned}
I_s^{\text{periodic}} &\simeq I_c \sin[\omega_0 t' - k_0 \sin(\theta_0 + \delta\theta_p(t')) \\
&\quad \times \sin(\omega_2 t' + \sin(\omega_1 t')/\omega_1 + \delta\phi_p(t'))] \quad (23)
\end{aligned}$$

where $\delta\theta_p$ and $\delta\phi_p$ are given by

$$\begin{aligned}\delta\theta_p &= -\frac{\epsilon_0}{2} \left[\sum_{n_1, n_2, n_3} J_{n_1}\left(\frac{1}{\omega_1}\right) J_{n_2}(k_0 \sin(\theta_0)) J_{n_3}\left(\frac{n_2}{\omega_1}\right) \sum_{s=\pm 1} \frac{\cos[\gamma_{00} + (\omega_0 - (n_3 + sn_1)\omega_1 - (n_2 + s)\omega_2)t'] - \cos(\gamma_{00})}{\omega_0 - (n_3 + sn_1)\omega_1 - (n_2 + s)\omega_2} \right] \quad (24) \\ \delta\phi_p &= \frac{\epsilon_0}{2} \cot(\theta_0) \left[\sum_{n_1, n_2, n_3} J_{n_1}\left(\frac{1}{\omega_1}\right) J_{n_2}(k_0 \sin(\theta_0)) J_{n_3}\left(\frac{n_2}{\omega_1}\right) \sum_{s=\pm 1} s \frac{\sin[\gamma_{00} + (\omega_0 - (n_3 + sn_1)\omega_1 - (n_2 + s)\omega_2)t'] - \sin(\gamma_{00})}{\omega_0 - (n_3 + sn_1)\omega_1 - (n_2 + s)\omega_2} \right]\end{aligned}$$

We note that the main contribution to the zeroth order results again comes from terms linear in time which occurs for

$$\omega_0 - (n_3^s + sn_1^s)\omega_1 - (n_2^s + s)\omega_2 = 0 \quad (25)$$

for $s = \pm 1$. The perturbation theory thus remain valid for $t \leq T_p'$ so that

$$\epsilon_0 T_p' J_{n_1^s}\left(\frac{1}{\omega_1}\right) J_{n_2^s}(k_0 \sin(\theta_0)) J_{n_3^s}\left(\frac{n_2^0}{\omega_1}\right) \leq 1. \quad (26)$$

The behavior of the DC component of I_s^{periodic} as a function of ϵ_0 , as obtained from Eq. 23 is discussed and compared to exact numerics in Sec. III.

External AC drive: Next, we consider the behavior of I_s in the presence of both an external magnetic field and an AC field of amplitude A and frequency ω_A so that $\gamma_0(t) = \alpha_0 + \omega_0 t' + A \sin(\omega_A t')/\omega_A$. First we consider a constant magnetic field for which $f(t') = 1$. In this case, using Eqs. 8 and 11, one obtains, to zeroth order in ϵ_0

$$\begin{aligned}I_s &\simeq I_c \sin \left[\omega_0 t' + A \sin(\omega_A t')/\omega_A \right. \\ &\quad \left. - k_0 \sin(\theta_0) \sin \omega_B t' + \gamma_{00} \right] \\ &\simeq I_c \sum_{n_1, n_2} J_{n_1}(A/\omega_A) J_{n_2}(k_0 \sin(\theta_0)) \\ &\quad \times \sin(\gamma_{00} + (\omega_0 + n_1 \omega_A - n_2 \omega_B)t') \quad (27)\end{aligned}$$

A finite DC component of I_s leading to Shapiro like steps thus appear in the I-V characteristics for integers n_1^0, n_2^0 which satisfies

$$\omega_0 + n_1^0 \omega_A - n_2^0 \omega_B = 0. \quad (28)$$

The condition of occurrence of these peaks mimics those for periodic magnetic field in the absence of external AC drive and the peak amplitude depends on the product of two Bessel functions. We note that the resultant Shapiro steps may occur for low AC drive frequencies and thus could, in principle, be amenable to easier experimental realization.

Next, we consider a periodically varying magnetic field in the presence of external radiation. In this case, one has, $f(t') = \omega_B + \cos(\omega_1 t')$. Using Eq. 8, one has $z(t') =$

$\omega_2 t' + \sin(\omega_1 t')/\omega_1$ which leads to (Eq. 11)

$$\begin{aligned}I_s &\simeq I_c \sin \left[\omega_0 t' + A \sin(\omega_A t')/\omega_A - k_0 \sin(\theta_0) \times \right. \\ &\quad \left. \sin(\omega_B t' + \omega_2 t' + \sin(\omega_1 t')/\omega_1 + \gamma_{00}) \right] \\ &\simeq I_c \sum_{n_1, n_2, n_3} J_{n_1}(A/\omega_A) J_{n_2}(k_0 \sin(\theta_0)) J_{n_3}(n_2/\omega_2) \\ &\quad \times \sin(\gamma_{00} + (\omega_0 + n_1 \omega_A - n_2(\omega_2 + \omega_B) - n_3 \omega_1)t')\end{aligned}$$

Thus the presence of the steps now occurs for a set of integers (n_1^0, n_2^0, n_3^0) which satisfies

$$\omega_0 + n_1^0 \omega_A - n_2^0(\omega_2 + \omega_B) - n_3^0 \omega_1 = 0. \quad (30)$$

The perturbative $O(\epsilon_0)$ corrections to the above solutions can be carried out in similar manner to that outlined above.

C. Dissipative nanomagnets

In this section, we include the Gilbert term in the LLG equations to model dissipative nanomagnets and seek a solution to these equations in the limit weak dissipation and weak coupling between the JJ and the nanomagnets. The resultant LLG equations are given by

$$\frac{d\vec{M}}{dt} = \gamma_g(\vec{M} \times \vec{B}_{\text{eff}}) - \frac{\eta\gamma_g}{M_0} \vec{M} \times (\vec{M} \times \vec{B}_{\text{eff}}) \quad (31)$$

Following the same parametrization as in Eqs. 6, we find that in terms of θ and ϕ , one can express the LLG equations, in terms of θ and ϕ , as

$$\begin{aligned}\frac{d\phi}{dt'} &= \omega_B(t') - \epsilon_0 \cot \theta \sin \phi \sin(\gamma_0(t') - k_0 \sin(\theta) \sin(\phi)) \\ \frac{d\theta}{dt'} &= \epsilon_0 \cos(\phi) \sin(\gamma_0(t') - k_0 \sin(\theta) \sin(\phi)) \\ &\quad - \eta \omega_B(t') \sin(\theta).\end{aligned} \quad (32)$$

where we have neglected terms $O(\epsilon_0 \eta)$. We note that the effect of the dissipative term manifests itself in θ but not in ϕ ; this fact can be understood as a consequence of the fact that to leading order $\vec{M} \times (\vec{M} \times \vec{B}_{\text{eff}})$ lies along \hat{y} and hence only effects the dynamics of M_y . For small ϵ_0 and η , Eq. 32 therefore admits a perturbative solution

$$\begin{aligned}\phi(t') &= z(t') + \delta\phi(t'), \quad \theta(t') = \delta\theta_d(t') \\ \delta\theta_d(t') &= 2 \arctan[\tan(\theta_0/2) e^{-\eta z(t')}] + \delta\theta(t').\end{aligned} \quad (33)$$

where $z(t')$, $\delta\theta(t')$, and $\delta\phi(t')$ are given by Eq. 8 and we have neglected terms $O(\epsilon_0\eta)$. The supercurrent, in the presence of the dissipative term is given by

$$I_s = I_c \sin[\gamma_0(t') - k_0 \sin(\theta_d(t')) \sin(\phi(t'))] \quad (34)$$

The fate of the DC component of I_s leading to Shapiro-like steps in the presence of the dissipative term shall be checked numerically in Sec. III for both periodic and constant applied magnetic fields.

III. NUMERICAL RESULTS

In this section, we analyze the coupled JJ-nanomagnet system both without and in the presence of dissipation

$$\begin{aligned} \frac{d\theta}{dt'} &= \epsilon_0 \cos \phi \sin(\gamma_0(t') - k_0 \sin \theta \sin \phi) - \eta[(\cos(\alpha_0)f(t') + K' \cos \theta) \sin \theta - f(t') \sin(\alpha_0) \cos \theta \cos \phi \\ &\quad - \epsilon_0 \sin \phi \cos \theta \sin(\gamma_0(t') - k_0 \sin \theta \sin \phi)] + \sin(\alpha_0)f(t') \sin \phi \\ \frac{d\phi}{dt'} &= (f(t') \cos(\alpha_0) + K' \cos \theta) - \epsilon_0 \cot \theta \sin \phi \sin(\gamma_0(t') - k_0 \sin \theta \sin \phi) \\ &\quad + \eta[-f(t') \sin(\alpha_0) \sin \phi (\sin \theta + \cos^2 \theta / \sin \theta) \\ &\quad + \epsilon_0 (\sin \theta \cos^3 \phi + \cos^2 \theta \cos \phi / \sin \theta + \sin \theta \cos \phi \sin^2 \phi) \sin(\gamma_0(t') - k_0 \sin \theta \sin \phi)] - f(t') \sin(\alpha_0) \cot \theta \cos \phi \end{aligned} \quad (35)$$

or cartesian variables $m_{x,y,z}$ which satisfies

$$\begin{aligned} \frac{dm_x}{dt'} &= -(f(t') \cos \alpha_0 + K' m_y) m_z + \epsilon_0 m_y \sin(\gamma_0(t') - k_0 m_z) - \eta[m_x m_y (f(t') \cos(\alpha_0) + K' m_y) \\ &\quad - f(t') \sin(\alpha_0) (m_y^2 + m_z^2) + m_x m_z \epsilon_0 (\sin(\gamma_0(t') - k_0 m_z))] \\ \frac{dm_y}{dt'} &= -\epsilon_0 m_x \sin(\gamma_0(t') - k_0 m_z) + \sin(\alpha_0) f(t') m_z - \eta[-(m_x^2 + m_z^2) (f(t') \cos(\alpha_0) + K' m_y) + f(t') \sin(\alpha_0) m_x m_y \\ &\quad + m_y m_z \epsilon_0 \sin(\gamma_0(t') - k_0 m_z)] \\ \frac{dm_z}{dt'} &= (f(t') \cos(\alpha_0) + K' m_y) m_x - \sin(\alpha_0) f(t') m_y - \eta[m_y m_z (f(t') \cos(\alpha_0) + K' m_y) + f(t') \sin(\alpha_0) m_x m_z \\ &\quad - (m_x^2 + m_y^2) \epsilon_0 (\sin(\gamma_0(t') - k_0 m_z))] \end{aligned} \quad (36)$$

In these equations $f(t') = 1$ for constant and $f(t') = \cos(\omega_1 t')$ for the periodically varying magnetic fields, $\alpha_0 = 0$ indicates an applied magnetic field along \hat{y} , we have set $\theta_0 = \pi/3$ and $\gamma_{00} = \pi/2$ for all simulations, and $K' = KM_0/B_1$. Note that Eqs. 35 and 36 reduces to the usual LL equations for $\eta = 0$. The supercurrent is then computed using the values of m_z obtained from Eqs. 35 or 36: $I_s = I_c \sin(\gamma_0(t') - k_0 m_z)$. We note that the choice between Eq. 35 and 36 is decided by numerical convenience; the final result turns out to be the same irrespective of which these equations are used.

To compare the theoretical results with exact numerics, we first compare the values $I_s(t')/I_c$ computed theoretically (Eq. 20) with exact numerical result. For comparing the two results, we have fixed the external voltage

and compare these results, wherever applicable, to the theoretical results obtained in Sec. II A. In what follows, we focus on cases of constant or periodically varying magnetic fields since Shapiro-step like features are expected to appear in the I-V characteristics of the JJ only for these protocols. The LLG equations for magnetization solved numerically to generate the data for the plots in this section either uses the polar variables θ and ϕ leading to

$\omega_0 = \omega_B$ which leads to a Shapiro step in the I-V characteristics of the JJ with $n^0 = 1$. As discussed in Sec. II B, one expects one of the perturbative terms to grow linearly in time in this case; the presence of this linear term is expected to invalidate the perturbative theoretical results for $t' > T' \sim \epsilon_0^{-1}$. In Fig. 2(a), we show the comparison between theoretical and numerical values of $I_s(t')/I_c$ at $t' > 2 \times 10^4 B_1^{-1}$ for $\epsilon_0 = 10^{-4}$; we find that the numerical and analytical values differ by less than 5% even at late times ($t \simeq 2T'$). In Fig. 2(b), we plot T' , which is the minimum time at which the deviation between theoretical and numerical values of $I_s(t')/I_c$ reaches 1% near the peak position, as a function of ϵ_0 ; the result shows the expected decrease of $T' \sim 1/\epsilon_0$ as ϵ_0 increases. In Fig. 3(a), we carry out a similar comparison for dissipative nano-

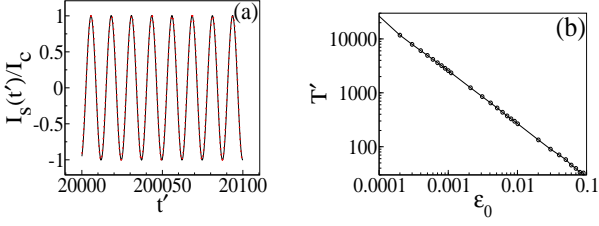


FIG. 2: (a) Comparison between theoretical (red dots) and numerical (black solid line) values of $I_s(t')/I_c$ as a function of time at late times $t' \geq 2 \times 10^4 B_1^{-1}$ for a constant magnetic field $\omega_B = 0.5$ along \hat{y} . Other parameters are $\epsilon_0 = 10^{-4}$, $\eta = 0$, $k_0 = 0.05$, $K = 0.0001$ and $\omega_0 = 0.5$. (b) Plot of time T' after which the theoretical and analytic results for $I_s(t)$ deviates by more than 1% at the peak position as a function of ϵ_0 .

magnets with $\eta = 0.0001$; we find that T' decreases with ϵ_0 in a qualitatively similar manner to the non-dissipative case. Finally, in Fig. 3(b), we plot T'_p for a periodically varying magnetic field with $\omega_1 = 1.2$. As expected from Eq. 26, $T'_p \sim 100\epsilon_0^{-1} \gg \epsilon_0^{-1}$ which implies much better stability for the Shapiro-like steps for periodic magnetic field compared to their constant field counterparts.

Next, we study the presence of a finite DC component of I_s in the case of a constant applied magnetic field along \hat{y} ($f(t') = 1$ and $\alpha_0 = 0$) in the absence of dissipation ($\eta = 0$) and external AC voltage ($\gamma_0(t') = \omega_0 t'$). The results of our study is shown in Fig. 4 where we plot I_s^{DC}/I_c , with I_s^{DC} given by

$$I_s^{\text{DC}} = \frac{1}{T_{\text{max}}} \int_0^{T_{\text{max}}} I_s(t') dt' = I_s(\omega = 0), \quad (37)$$

as a function of ω_0 for a fixed constant ω_B . Here

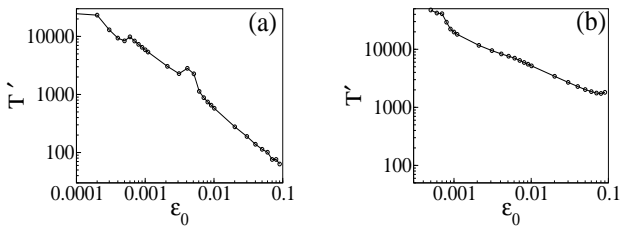


FIG. 3: (a) Plot of T' as a function of ϵ_0 for $\eta = 0.0001$. (b) Plot of T' as a function of ϵ_0 for periodic protocol with $\omega_B = 0$, $\eta = 0$, and $\omega_1 = 1.2$. All other parameters are same as in Fig. 2.

$T_{\text{max}} = 40,000$ represents the maximum time up to which we average $I_s(t')$. Note that $I_s(t')$ is chosen so that increasing it any further does not lead to a change in the peak height for $\epsilon_0 = 0$. As shown in Fig. 4(a), (b) and (c), we find that for $\epsilon_0 \ll 1$, I_s^{DC} shows sharp peaks at $\omega_0 = \omega_B, 2\omega_B$ corresponding to $n^0 = 1, 2$ in Eq. 18; the position of this peaks match exactly with our theoretical results. However, the peak heights turn out to be

smaller than that predicted by theory and they rapidly decrease with increasing ϵ_0 . This mismatch between theoretical and numerical results is a consequence of the linearly growing perturbative terms $\sim \epsilon_0$ in expression for $\delta\theta(t')$ and $\delta\phi(t')$ (Eq. 19) which invalidate the theoretical result for $T' \sim \epsilon_0^{-1}$. Thus for constant magnetic field and moderate $\epsilon_0 > 0.01$, the step-like feature predicted in Eq. 18 disappears. In Fig. 4(d), we study the behavior of the peak with variation of α_0 . We find that the height of the peak increases with α_0 for small α_0 in accordance with the theoretical prediction of Sec. II A. For larger $\alpha_0 > \alpha_0^{\text{max}}$, the peak height starts to decrease and the peak height becomes almost half of its maximum for $\alpha_0 = \pi/2$ when $\vec{B} \parallel \hat{x}$.

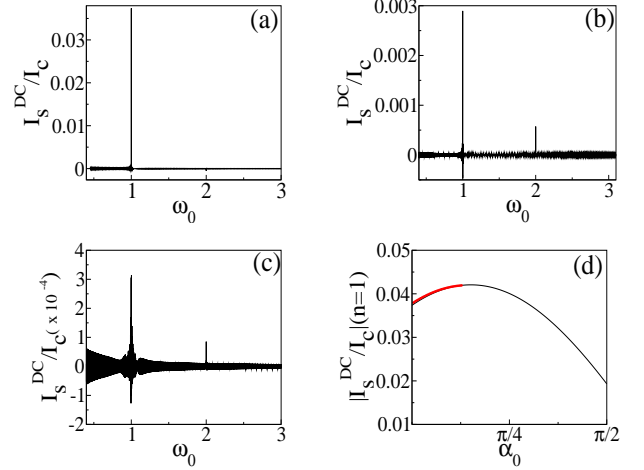


FIG. 4: Plot $I_s(\omega = 0)/I_c \equiv I_s^{\text{DC}}/I_c$ as a function of the Josephson frequency $\omega_0 = 2eV_0/(\hbar\gamma_g B_1)$ for a constant magnetic field $\omega_B \simeq 1$ with $K = 0.0001$, $k_0 = 0.1$ and (a) $\epsilon_0 = 0.0001$ (b) $\epsilon_0 = 0.001$ and (c) $\epsilon_0 = 0.01$. The position of the peaks corresponds to $n^0 = 1$ and $n^0 = 2$ as predicted by theoretical analysis. (d) Plot of the peak height for the $n^0 = 1$ peak as a function of the angle α_0 made by \vec{B} with \hat{y} for $\epsilon_0 = K = 0.0001$ and $k_0 = 0.1$. The red dots correspond to results from perturbative theoretical analysis near $\alpha_0 = 0$.

Next, we study the characteristics of the peaks in I_s^{DC} for periodically varying magnetic field for which $f(t') = \cos(\omega_1 t')$. In Figs. 5(a), (b), and (c), we plot I_s^{DC}/I_c as a function of ω_1 for a fixed $\omega_0 = 1.2$, $\alpha_0 = \omega_2 = \eta = 0$, and for several values of ϵ_0 . We find that the position of the peaks corresponds to integer values of n_2^0 (as indicated in the caption of Fig. 5) in complete accordance with Eq. 22 with $\omega_2 = 0$. Moreover, in contrast to the constant magnetic field case, the peaks of I_s^{DC} are much more stable against increasing ϵ_0 . This features of the peaks can be understood as follows. For periodic magnetic field with $\omega_2 = 0$, the zeroth order solution is given by $z(t') = \sin(\omega_1 t')/\omega_1$; thus the perturbative terms $\delta\theta(t')$ and $\delta\phi(t')$ (Eq. 24) involve product of Bessel functions. This renders the effective perturbative parameter to be $\epsilon_0^{\text{eff}} \simeq \epsilon_0 J_{n_1^s}(\frac{1}{\omega_1}) J_{n_2^s}(k_0 \sin(\theta_0)) J_{n_3^s}(\frac{n_2^0}{\omega_1})$

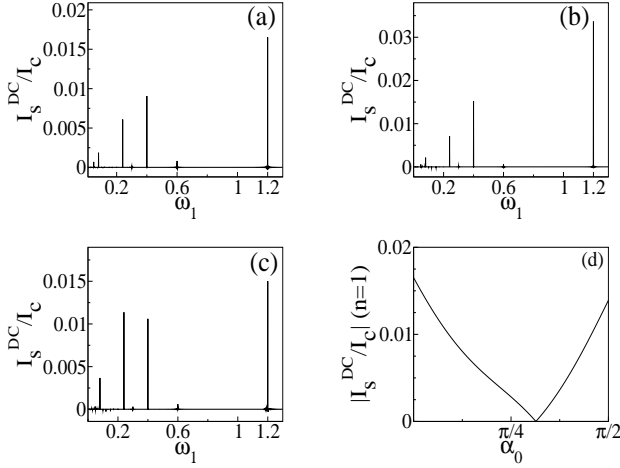


FIG. 5: Plot I_s^{DC}/I_c for a periodically varying magnetic field $B = B_1 \sin \omega_1 t$ as a function of ω_1 with $K = 0.0001$, $k_0 = 0.1$, $\omega_0 = 1.2$ and (a) $\epsilon_0 = 0.0001$ (b) $\epsilon_0 = 0.001$ and (c) $\epsilon_0 = 0.01$. The position of the peaks corresponds to $n_2^0 = 1, 2, 3, 4$ (from right to left) as predicted by theoretical analysis. (d) Plot of the peak height for the $n_2^0 = 1$ peak as a function of the angle α_0 made by \vec{B} with \hat{y} for $\epsilon_0 = K = 0.0001$ and $k_0 = 0.1$.

(Eqs, 25 and 26). Consequently, the effect of the perturbative correction to the weak coupling solution is drastically reduced in this case leading to a better stability of peak height with increasing ϵ_0 . Thus periodic magnetic fields are expected to lead to enhanced stability of Shapiro steps compared to their constant field counterparts. Finally in Fig. 5 (d), we show the variation of the peak height of I_s^{DC} as a function of α_0 . We again

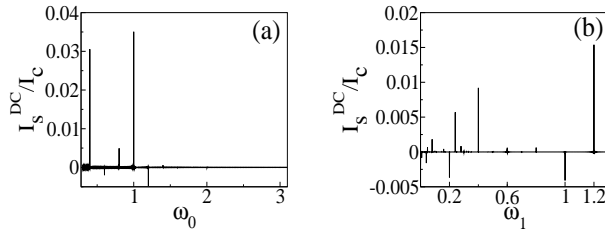


FIG. 6: (a) Plot of I_s^{DC}/I_c in the presence of an AC field $\omega(t') = \omega_0 + A \sin(\omega_A t')/\omega_A$ with $A = 0.1$, $\omega_A = 0.2$, $\epsilon_0 = K = 0.0001$, $k_0 = 0.1$ as a function of ω_0 for constant magnetic field $\omega_B = 1$. (b) Similar plot as a function of ω_1 for periodic magnetic field with $\omega_0 = 1.2$. All the peak positions conform to the theoretical prediction in Sec. II B.

find similar non-monotonic behavior of the peak height as a function of α_0 ; the reason for this is similar to that already discussed in the context of constant magnetic field case. However, in the present case, the correction terms are much smaller and the peak height is accurately predicted by the zeroth order perturbative results: $I_s^{\text{DC}}/I_c \sim 2J_{n_1^0}(k_0 \sin(\theta_0 - \alpha_0))J_{n_2^0}(n_1^0/\omega_1)$. This is most easily checked by noting that the peak height vanishes

ω_1	n_1^0	n_3^0	ω_1	n_1^0	n_3^0
1.2	0	1	0.3	0	4
1	-1	1	0.28	1	5
0.8	2	2	0.24	0	5
0.6	0	2	0.2	-3	3
0.4	-2	2	0.2	0	6
0.4	0	3	0.08	0	15

TABLE I: Tabulated values of n_1^0 and n_3^0 for all the peaks that appear in Fig. 7(b) at specific ω_1 values listed above. Note that n_2^0 does not appear in the table since the peaks correspond to $\omega_B = 0$ so that their position are independent of n_2^0 (Eq. 30).

for $\alpha_0 = \theta_0 = \pi/3$ for which $J_{n_1^0}(0) = \delta_{n_1^0,0}$ leading to vanishing of the peak for $n_2^0 = 1$.

Next, we study the behavior of the system in the presence of an applied AC field of amplitude A and frequency ω_A . In the presence of such a field $\omega(t') = \omega_0 + A \sin(\omega_A t')/\omega_A$. In Fig. 6(a), we show the behavior of the peaks of I_s^{DC} as a function of ω_0 for a fixed $\omega_A = 0.2$ and $A = 0.1$ in the presence of a constant magnetic field. The peaks in I_s^{DC} occur at $\omega_0 = 0.4, 0.6, 0.8, 1$ (from left to right); each of these correspond to two sets of $(n_1^0, n_2^0) = (3, 1)$ and $(-2, 0)$, $(2, 1)$ and $(-3, 0)$, $(1, 1)$ and $(-4, 0)$ and $(0, 1)$ and $(-5, 0)$ respectively as predicted in Eq. 28. In Fig. 6(b), we investigate the behavior for I_s^{DC} for a periodically varying magnetic field as a function of ω_1 for $\omega_0 = 1.2$ and for same amplitude and frequency of the AC field. We find several peaks in I_s^{DC} ; each of these peaks corresponds to a fixed set of integers (n_1^0, n_3^0) (Eq. 30 with $\omega_2 = 0$) as shown in Table I.

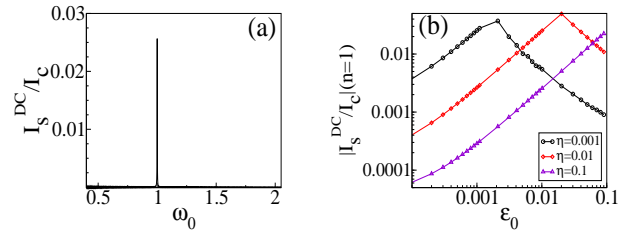


FIG. 7: (a) Plot of I_s^{DC}/I_c for a constant applied magnetic field as a function of ω_0 with $\eta = 0.0001$. All other parameters are same in Fig. 4(a). (b) Variation of the peak height (for $n^0 = 1$) as a function of ϵ_0 for $\eta = 0.001$ and 0.1 showing the presence of an optimal ϵ_0 for which the peak height is maximal.

Next, we study the effect of dissipation on these peaks by plotting I_s^{DC} as a function of ω_0 in Fig. 7(a) (for constant magnetic field) and as a function of ω_1 in Fig. 8(a) (periodic magnetic field) for $\eta = 0.0001$. As seen in both cases, the position of the peaks remain same as that for $\eta = 0$ in accordance with the analysis of Sec. II C. The variation of the peak height as a function of ϵ_0 for sev-

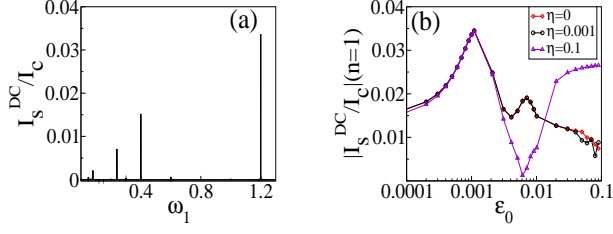


FIG. 8: (a) Plot of I_s^{DC}/I_c for a periodically varying magnetic field as a function of ω_1 with $\eta = 0.0001$. All other parameters are same in Fig. 5(b). (b) Variation of the peak height (for $n_0 = 1$) as a function of ϵ_0 for $\eta = 0, 0.001$ and 0.1 showing the presence of an optimal ϵ_0 for which the peak height is maximal.

eral representative values of η is shown in Figs. 7(b) and 8(b). We find that the peak height is maximal when $\eta \simeq \epsilon_0$. This feature can be understood from the fact that for small η , the term in $\delta\theta_d$ which varies linearly in time is minimal when $\eta \simeq \epsilon_0$; this leads to enhanced peak height as one approaches this value of η . Thus we find that the presence of dissipation in a nanomagnet leads to enhancement of the Shapiro-like steps for $\eta \sim \epsilon_0$.

Finally, before ending this section, we briefly study the effect of increasing T_{max} in our numerical study. The relevance of this lies in the fact that for any finite ϵ_0 and η , our analytical results hold till $t \sim T'$ (constant magnetic field) or $t \sim T'_p$ (periodic magnetic field) while the DC signal receives contribution from all T . Thus it is necessary to ensure that these deviations do not lead to qualitatively different results for the DC response. To this end, we plot the height of the peak value of I_s^{DC} as a function of $1/T_{\text{max}}$ in Fig. 9. We find from Fig. 9(a) that for constant magnetic field, the peak height indeed extrapolates to zero indicating that the Shapiro steps will be destabilized due to perturbative corrections if I_s is averaged over very long time. However, we note from Fig. 9(c), I_s^{DC} could retain a non-zero value in the presence of a finite dissipation parameter η . This could be understood since the effect of damping, as shown in Fig. 8, negates that of ϵ_0 on the peak value of I_s^{DC} . Furthermore, from Figs. 9(b) and (d), we note that for the periodic magnetic fields the extrapolated value of I_s^{DC} is a finite which is lead to finite Shapiro steps in the I-V characteristics of these JJs. Thus we expect that the Shapiro-step like features in the I-V characteristics of the JJ to be much more stable for periodically varying magnetic fields.

IV. DISCUSSION

In this work, we have studied a coupled JJ-nanomagnet system and analyzed the behavior of the supercurrent in the JJ in the presence of a finite coupling to the nanomagnet. We have provided a perturbative analytical solution to both the LL and the LLG equations governing the magnetization dynamics of the nanomagnet for arbitrary

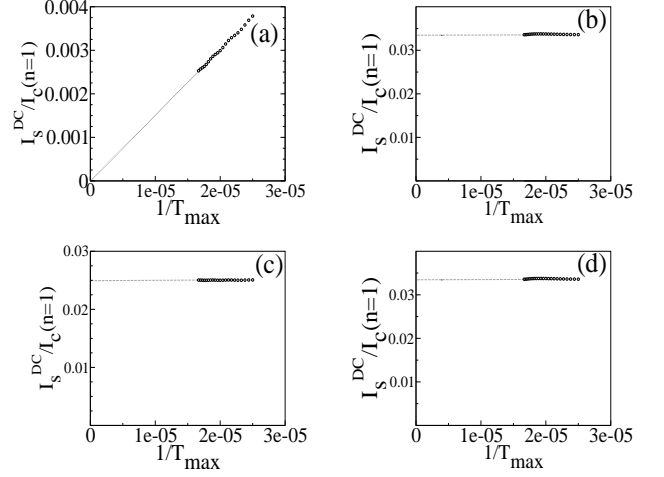


FIG. 9: Plot I_s^{DC}/I_c as a function of $1/T_{\text{max}}$ for (a) constant magnetic field with $\epsilon_0 = 0.001$ and $\eta = 0$, (b) periodically varying magnetic field with $\epsilon_0 = 0.001$ and $\eta = 0$, (c) constant magnetic field with $\epsilon_0 = \eta = 0.001$ and (d) Periodically varying magnetic field with $\epsilon_0 = \eta = 0.001$. All other parameters are same as in Figs. 4 and 5.

time-dependent magnetic field applied along the easy axis of the nanomagnet in the presence of weak coupling to the JJ and for weak dissipation. We have estimated the regime of validity of our perturbative results.

Using these results, we have studied the behavior of the supercurrent of the JJ for constant and periodically varying magnetic fields. The reason for choice such magnetic fields are that they are the only ones which lead to a fixed DC component of $I_s(t)$ which in turn leads to Shapiro step-like features in the I-V characteristics of the JJ. We note that while such features are known for constant magnetic field from earlier works^{16,17}, the presence of such peaks in I_s^{DC} has not been theoretically reported for periodically varying magnetic fields. Moreover, we show, both from our analytical results and by performing exact numerics which supports these results, that the peaks in I_s^{DC} for periodically varying magnetic field are much more robust against increase of both ϵ_0 and η compared to their constant field counterparts; we therefore expect such peaks to be more experimentally accessible. We have also studied the behavior of such JJ-nanomagnet systems in the presence of external AC voltage. The presence of such a voltage leads to more peaks in I_s^{DC} whose positions are accurately predicted by our theoretical analysis.

The experimental verification our work would involve preparing a JJ-nanomagnet system with sufficiently small values of ϵ_0 . For this we envisage a 2D thin film superconducting junction in the $x - y$ plane coupled to the nanomagnet as shown in Fig. 1. We note that value of Josephson energy in a typical niobium film is $E_J \sim 40\text{K}$. Thus for a typical magnetic field $\simeq 100$ Gauss, one could estimate an $\epsilon_0 \simeq 0.0005$ for $k_0 \simeq 0.1$. Moreover the critical current in such junctions is $I_c = 2eE_J/\hbar \simeq 1.5\mu\text{A}$.

Thus the peaks in DC would correspond to $I_s^{\text{DC}} \simeq 10\text{nA}$ which is well within detection capability of standard experiments.

To conclude, we have provided a perturbative analytic results for supercurrent of a coupled JJ-nanomagnet system in the limit of weak coupling between them and in the presence of a time dependent field applied to the system. Using this analytic result and exact numerical solution of the LL and the LLG equations, we predict existence of peaks in I_s^{DC} for both constant and periodic magnetic fields which are expected to provide Shapiro-

like steps in the I-V characteristics of the JJ without the presence of external AC drive. We have analyzed the effect of finite dissipation of the nanomagnet and the presence of external AC drive on these peaks and discussed experiments which can test our theory.

Acknowledgement: KS acknowledges DST/RFBR grant INT/RUS/RFBR/P-249. RG acknowledges SPM fellowship from CSIR for support. The reported study was partially funded by RFBR according to the research projects 15-29-01217 and 16-52-45011, India.

-
- ¹ K. K. Likharev, Rev. Mod. Phys. **51**, 101 (1979); K. K. Likharev, *Dynamics of Josephson Junctions and Circuits*, (Taylor and Francis, London, 1986).
 - ² A. Kitaev, Phys. Usp. **44**, 131 (2001).
 - ³ H-J Kwon, K. Sengupta, V.M. Yakovenko, Eur. Phys. J. B **37**, 349 (2004).
 - ⁴ R. M. Lutchyn, J. D. Sau, and S. Das Sarma, Phys. Rev. Lett. **105**, 077001 (2010); Y. Oreg, G. Refael, and F. von Oppen, Phys. Rev. Lett. **105**, 177002 (2010).
 - ⁵ L. Fu and C. L. Kane, Phys. Rev. Lett. **100**, 096407 (2008). [9] L. Fu and C. L. Kane, Phys. Rev. B **79**, 161408(R) (2009); J. D. Sau, R. M. Lutchyn, S. Tewari, and S. Das Sarma, Phys. Rev. Lett. **104**, 040502 (2010); J. Alicea, Phys. Rev. B **81**, 125318 (2010); A. Cook and M. Franz, Phys. Rev. B **84**, 201105(R) (2011); J. D. Sau and S. D. Sarma, Nat. Commun. **3**, 964 (2012); A. Das, Y. Ronen, Y. Most, Y. Oreg, M. Heiblum, and H. Shtrikman, Nat. Phys. **8**, 887 (2012); M. T. Deng, C. L. Yu, G. Y. Huang, M. Larsson, P. Caroff, and H. Q. Xu, Nano Lett. **12**, 6414 (2012); A. D. K. Finck, D. J. Van Harlingen, P. K. Mohseni, K. Jung, and X. Li, Phys. Rev. Lett. **110**, 126406 (2013); H. O. H. Churchill, V. Fatemi, K. Grove-Rasmussen, M. T. Deng, P. Caroff, H. Q. Xu, and C. M. Marcus, Phys. Rev. B **87**, 241401 (2013); M. Cheng and R. M. Lutchyn, Phys. Rev. B **92**, 134516 (2015).
 - ⁶ L. P. Rokhinson, X. Liu, and J. K. Furdyna, Nat. Phys. **8**, 795 (2012); V. Mourik, K. Zuo, S. M. Frolov, S. R. Plissard, E. P. A. M. Bakkers, and L. P. Kouwenhoven, Science **336**, 1003 (2012); W. Chang, V. E. Manucharyan, T. S. Jespersen, J. Nygard, and C. M. Marcus, Phys. Rev. Lett. **110**, 217005 (2013); S. Nadj-Perge, I. K. Drozdov, J. Li, H. Chen, S. Jeon, J. Seo, A. H. MacDonald, B. A. Bernevig, and A. Yazdani, Science **346**, 602 (2014); E. J. H. Lee, X. Jiang, M. Houzet, R. Aguado, C. M. Lieber, and S. D. Franceschi, Nat. Nanotechnol. **9**, 79 (2014).
 - ⁷ S. Shapiro, Physical Review Letters **11**, 80 (1963).
 - ⁸ M. Houzet, J. S.Meyer, D.M. Badiane, and L. I. Glazman, Phys. Rev. Lett. **111**, 046401 (2013); L. Jiang, D. Pekker, J. Alicea, G. Refael, and Y. Oreg, and F. von Oppen, Phys. Rev. Lett. **107**, 236401 (2011); F. Dominguez, F. Hassler, and G. Platero, Phys. Rev. B **86**, 140503 (2012); D. I. Pikulin and Y. V. Nazarov, Phys. Rev. B **86**, 140504(R) (2012); J. D. Sau, E. Berg, and B. I. Halperin, arXiv:1206.4596 (unpublished).
 - ⁹ M. Maiti, K. M. Kulikov, K. Sengupta, and Yu. M. Shukrinov, Phys. Rev. B **92**, 224501 (2015).
 - ¹⁰ We note that, as shown in Ref. 9, odd subharmonic steps can occur in these junction for a wide range of dissipation parameter in the presence of finite junction capacitance.
 - ¹¹ I. O. Kulik, Zh. Eksp. Teor. Fiz. **49**, 585 (1966) [Sov. Phys. JETP **22**, 841 (1966)].
 - ¹² L. N. Bulaevskii, V. V. Kuzii, and A. A. Sobyenin, Zh. Eksp. Teor. Fiz. **25**, 314 (1977) [JETP Lett. **25**, 290 (1977)].
 - ¹³ J.-X. Zhu, Z. Nussinov, A. Shnirman, and A. V. Balatsky, Phys. Rev. Lett. **92**, 107001 (2004); Z. Nussinov, A. Shnirman, D. P. Arovas, A. V. Balatsky, and J. X. Zhu, Phys. Rev. B **71**, 214520 (2005).
 - ¹⁴ C. Padurariu and Yu. V. Nazarov, Phys. Rev. B **81**, 144519 (2010).
 - ¹⁵ L. Dell'Anna, A. Zazunov, R. Egger, and T. Martin, Phys. Rev. B **75**, 085305 (2007).
 - ¹⁶ L. Cai and E.M. Chudnovsky, Phys. Rev. B **82**, 104429 (2010); L. Cai, D. A. Garanin, and E. M. Chudnovsky, Phys. Rev. B, **87**, 024418 (2013).
 - ¹⁷ A. I. Buzdin, Rev. Mod. Phys. **77**, 935 (2005); A. Buzdin, Phys. Rev. Lett. **101**, 107005 (2008); F. Konschelle and A. Buzdin, Phys. Rev. Lett. **102**, 017001 (2009); Yu M. Shukrinov, I. R. Rahomonov, K. Sengupta, and A. Buzhdin, arXiv:1702.08394 (unpublished).
 - ¹⁸ W. Wernsdorfer, Adv. Chem. Phys. **118**, 99 (2001); W. Wernsdorfer, Supercond. Sci. Technol. **22**, 064013 (2009).
 - ¹⁹ C. Thirion, W. Wernsdorfer, and D. Mailly, Nat. Mater. **2**, 524 (2003).